LOAD-BEARING MULTI-FUNCTIONAL STRUCTURE WITH DIRECT THERMAL HARVESTING FOR THERMALLY ACTIVATED RECONFIGURABLE WING DESIGN

J. Joo[1*], B. Smyers[1], R. Beblo[2], G. Reich[1]
[1] Air Force Research Laboratory, Wright-Patterson AFB, Ohio, USA,
[2] University of Dayton Research Institute, Dayton, Ohio, USA
* Corresponding author (james.joo@wpafb.af.mil)

Keywords: *Reconfigurable wing, UAV, Shape memory polymer, Thermal energy harvesting, Multifunctional structure, Compliant mechanism*

1 Introduction

Reconfigurable structures such as morphing aircraft are multidisciplinary systems that require efficient integration of actuation, mechanisms, and structures to achieve the desired functionality by changing the state of the vehicles. Typically, the actuation requires an on-board energy source that reduces either the available payload or the vehicle's endurance, or both. In this case, the ability to operate in response to environmental change requires radically new structural concepts for system level capability. This paper seeks to understand new concepts that utilize heat from skin friction to trigger reconfiguration and employ a fundamental bi-stable effect of compliant mechanisms for shape change. Direct utilization of thermal energy helps to decrease the losses associated with energy conversion and passive activation using thermal energy can reduce the weight penalty by eliminating complicated control systems and separate actuators and it is reliable in the long term.

This paper describes a reconfigurable system and component designs of high-speed delivery of a low-speed Intelligence Surveillance Reconnaissance (ISR) asset (Fig. 1). The research focuses on investigating harvesting, transport, and usage of heat energy developed on the surface of the ISR pod with a blunt fuselage shape. A compliant mechanism is designed to change its configuration by deploying a folded wing as the induced heat load soften elements to reach an unfolded stable position. The size and shape of the mechanism are explored and the heating and material selection of the flexible link is discussed including overall energy efficiency of the system.

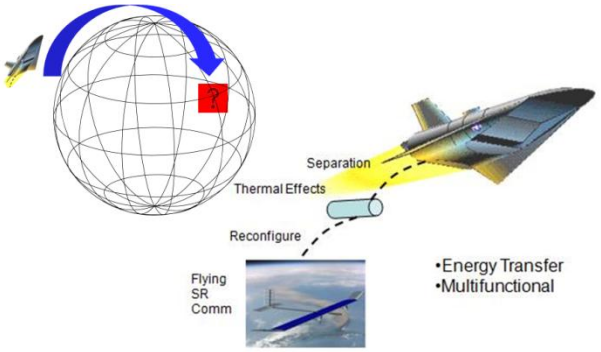

Fig. 1. Operational overview of a notional ISR delivery system [1]

2 System Design

A conceptual reconfigurable system proposed in this paper is shown in Fig. 2. It is composed of a thermal transport system (pod nose heat collector/conductor,

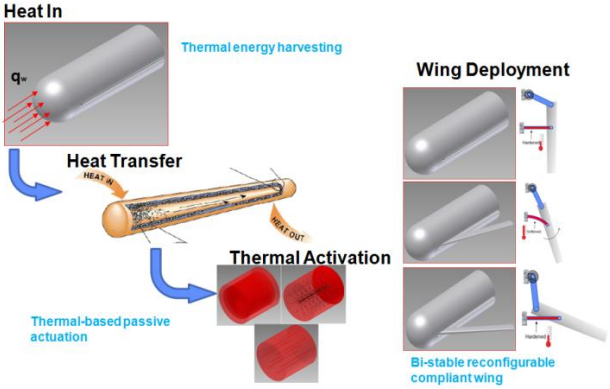

Fig. 2. Thermally activated reconfigurable system

heat pipe, and heat conductor in the flexible link) and passive reconfiguration system (Fig. 3) using a bi-stable compliant mechanism and a multi-phase material such as Shape Memory Polymer (SMP). The energy input/output, efficiency, usage, and transmission by each element is tracked and used to evaluate and optimize the performance of both the system and individual components. SMP is utilized as a variable stiffness link for the bi-stable mechanism. SMP provides thermal storage, damping, passive actuation, and load-bearing structure in this application. Fig. 4 shows the total potential energy plot as the Young's modulus of the SMP link changes with thermal load input. Since the mechanism is bi-stable, it shows two stable positions at 0° (deployed state) and ~60° (packaged state) but the second stable position disappears as the magnitude of the Young's modulus decreases as the SMP reaches its glass transition temperature. As soon as the second stable position (packaged state) disappears the mechanism jumps to the other stable position (deployed state) without any external load, which drives the passive reconfiguration of the system. VeriflexE has a reported glass transition temperature of 104ºC and approximate Young's moduli of 3.26GPa and 1.69MPa at 25ºC and 130ºC respectively [3,4]

3 Test Rig

To determine feasibility of the concept, a bench top test rig of the reconfigurable system was developed (Fig. 5). The demonstrator consists of 0.0127m diameter cylindrical samples made of neat or

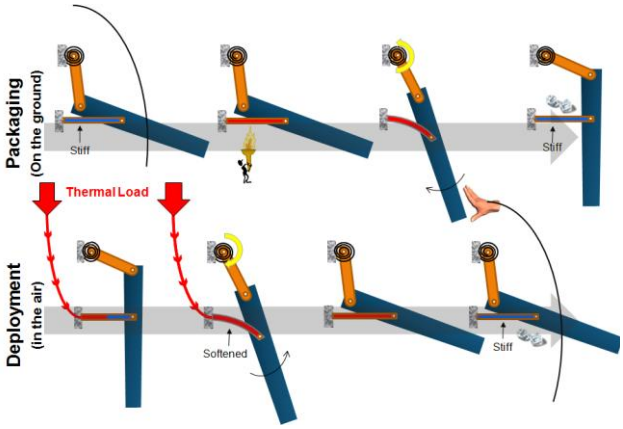

Fig. 3. Reconfiguration process

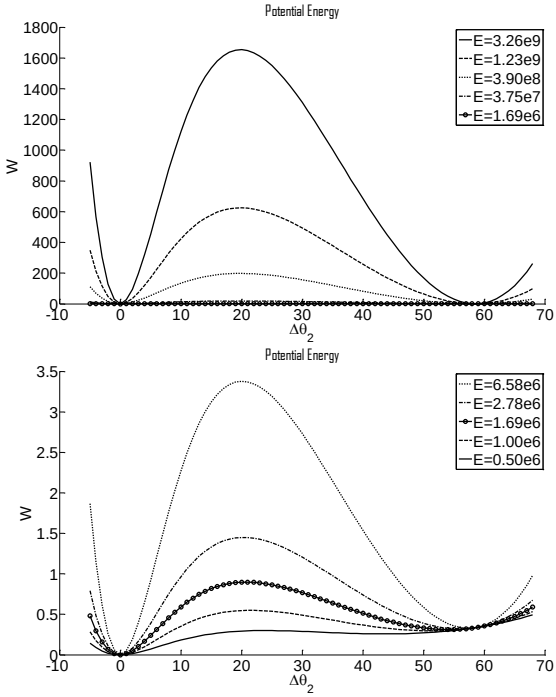

Fig. 4. Potential energy with respect to input angle for different Young's modulus of the flexible link (equations from [1])

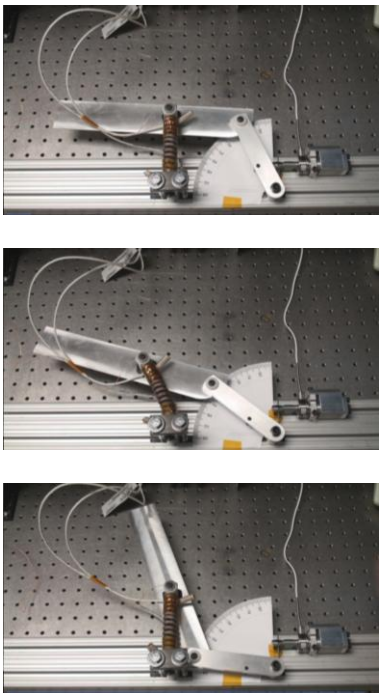

Fig. 5. A bi-stable compliant wing test rig

magnetite doped SMP links and wing components manufactured from aluminum, bearings, a heating element (Nichrome heater connected to a 90V power source), a torsional spring, and a load cell. Three imbedded conductor designs were previously developed to distribute thermal load in SMP link but were not implemented at this time. Instead, the cylindrical SMP link is wrapped with a Nichrome heater so that heat is conducted from the outside to the center of the link (Fig. 6). The mechanism is assembled with pin and bearing joints to minimize friction. The mechanism is mounted to a modular T-slot framing which allows for adjustment and the ability to scale up the demonstrator. When the wing is in the folded stable position the torsional spring is in a compressed state. The SMP is heated to approximately 100°C at which time the link softens, allowing the spring to act on the mechanism causing the wing to deploy and attain the second of the bi-stable positions.

Fig. 7 is an enlarged version of Fig. 4 around $\Delta\theta_2$ equal to 64º, the packaged state, created using test measurement. Each line in Fig. 7 represents the system potential energy at any given angle at a specified link Young's modulus. The minimum energy position, and thus the desired position of the mechanism, is indicated by circles. In the stiff state the modulus of the link is 3.26e9 Pa and the energy required to move the system away from the equilibrium position is substantial. As thermal energy is added to the link and the temperature increases; the modulus of the link decreases. As the modulus decreases, the energy curve of the system changes and the minimum energy state decreases in both energy and input angle. As the position of minimum energy moves, the input arm of the mechanism rotates to remain in the lowest possible energy state. The path of the experimental mechanism can then be traced by the circles in Fig. 7. As stated previously, as the temperature of the link approaches T_g, the angle of minimum energy approaches 0, resulting in the mechanism approaching the deployed position.

4 Thermal Energy

A hyper-sonic carrier deploys a mid-size ISR near orbit and the heat energy generated by the skin friction is calculated at a deployment speed and altitude of Mach 5 and 30 km [1]. After deployment, integrating over the entire trajectory, 3.3 MJ enters the heat pipe, and approximately 2.0 MJ is transferred to and absorbed by the flexible link, representing a thermal efficiency of 61% for a given trajectory neglecting energy loss from the heat collector (Fig. 8) [2]. Other modeled trajectories were found to have efficiencies higher than 80%. Due to difficulties in fabrication of an optimal heat collector (the design of which is described previously [1]), the efficiency of the heat collector was assumed. The remainder of the energy is utilized to raise the temperature of the components, and thus not transferred to the flexible link during

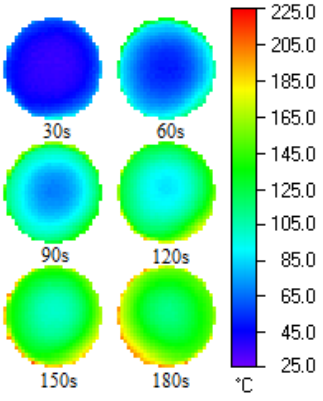

Fig. 6. IR images of cylindrical sample of neat VeriflexE. Pictures taken every 30 sec for three minutes (A Mikron Thermo Tracer TS7302 IR camera)

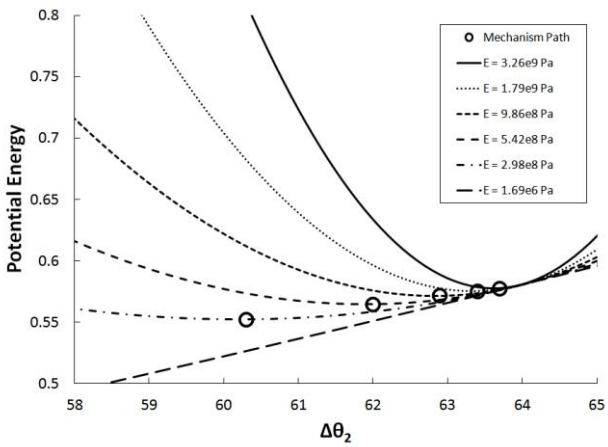

Fig. 7. Thermal initiation of mechanism morphing

the prescribed flight time. The thermal energy transferred to the flexible link is used to heat up the SMP to reduce its modulus. Some energy will be lost in this process because the thermal energy may not be evenly distributed over the link due to low conductivity/heat diffusivity of the SMP and the conductor design. The excessive temperature over the glass transition is considered redundant. Fig. 9 shows the efficiencies of each component of the system and available energies are described based on the test results. Thermal energy harvested from the environment was scaled down to laboratory level in this diagram. Considering energy loss at each step of the process, 37% of the harvested energy is used to heat the SMP link for reconfiguration. Note that no other losses are considered in this analysis, such that this number represents an upper bound on the amount of energy that can be utilized. Also, direct transfer of high quality thermal energy decreases the losses associated with energy conversion devices such as thermoelectric modules and ultimately increases the available energy to do useful work.

5 Magnetite (Fe_3O_4) doped Flexible Link

The magnetite nanoparticles used in the presented study were supplied by SkySpring Nanomaterials, Inc., product #3220DX. The iron oxide particles are 98% 20-30 nm diameter approximate spheres while the SMP used as the matrix material is the epoxy based SMP VeriflexE by Cornerstone Research Group, LLC.

The SMP resin was mixed per the manufacturer

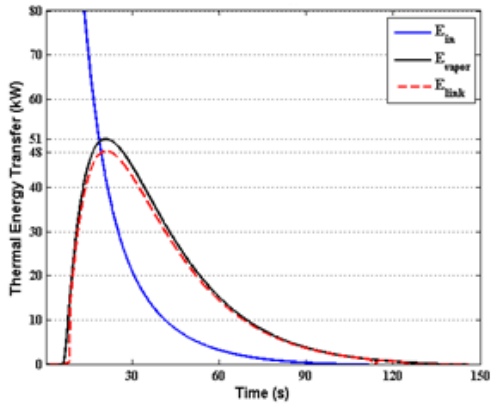

Fig. 8. Thermal energy transmission by the heat pipe [2]

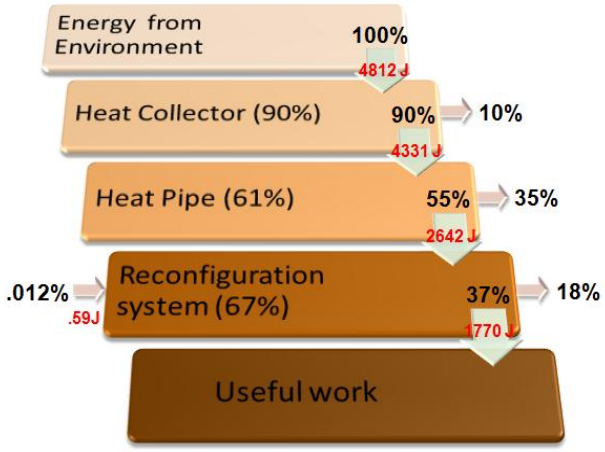

Fig. 9. System energy diagram

instructions and 10 wt% Fe_3O_4 particles mixed in by hand, with all components weighed by a Mettler Toledo benchtop scale to an accuracy of ± 0.05 g. Since the liquid uncured resin of VeriflexE has a measured density of approximately 1.153 g/cm^3 and using a density of 5.1 g/cm^3 [5] for magnetite, a 10 wt% composite of magnetite and VeriflexE is approximately 2.5 vol% particles. The SMP/magnetite composite is then left under medium vacuum (~25″ Hg) for approximately 10 minutes to remove air bubbles introduced during mixing. The mixture is then poured into a split cylindrical mold treated with Slide Epoxease mold release with the two halves sealed with Dow Corning 3145 RTV sealant and held together with standard hose clamps. The mold is then placed back under vacuum for an additional 5 minutes. The ends of the mold are sealed with Teflon® plugs and RTV and the sample cured in a laboratory oven per the manufacturer's suggested temperature cycle. After curing, the sample is de-molded and a hole drilled in one end for installation in the test setup.

Thermal properties of both neat VeriflexE and the SMP/magnetite composite are measured using a Hot Disk Thermal Constants Analyser TPS2500S from ThermTest Inc. accurate to ± 5%. Two cylindrical samples 0.5″ in diameter and 0.25″ in height are polished and a 4 mm diameter probe sandwiched between them to conduct the tests. The tests are conducted with the samples in a controlled thermal bath after a constant temperature for at least 5 minutes is attained. Thermal properties of both

specimens were measured at ambient (20°C). Results of the thermal properties tests are shown below in Table 1 and are used in calculating the energies and other analysis throughout the work.

Table 1: Thermal properties of samples measured at 20°C

	Neat Veriflex E	VeriflexE w/ 10wt% Fe_3O_4	Fe_3O_4
K (W/mK)	0.206	0.215	3.4 – 5.1 **
C_p (J/m^3K)	1.43e6	1.46e6	3.17e6 – 3.60e6 ***
α (m^2/s)	1.45e-7	1.47e-7	9.43e-7 – 1.61e-6

** References 5-7
*** References 8-10

6 Fabrication Issues

Fig. 10 shows the torque supplied to the input arm of the mechanism by a torsional spring. As with the time evolution of the angle of the input the torque is relatively constant for both the neat VeriflexE and magnetite composite samples until the temperature of the link approaches Tg, allowing the mechanism to rotate thus reducing the torque. The nominal increase in thermal diffusivity of the magnetite composite over the neat polymer results in a slight decrease in the time required for the link to reach the transition temperature, decreasing the time required for mechanism reconfiguration by approximately 5 seconds. Since doping magnetite in the SMP did not improve the thermal conductivity or diffusivity of the flexible link as expected, a Scanning Electron Microscope (SEM) micrograph is taken to investigate the distribution of the particles in the composite. In Fig. 11 the groups of particles are observed in various sizes from 10 to 20 μm across. Assuming the size of one particle is around 30nm as indicated by the manufacturer the aggregates are about 330 particles in diameter. Presumably, there is no SMP inside the clusters, resulting in voids or inclusions that would inhibit thermal transfer.

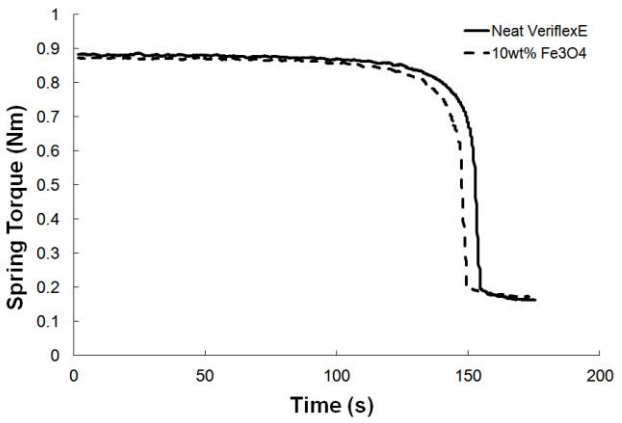

Fig. 10. Time evolution of spring torque

The way to resolve this issue is to disperse the particles in Acetone in a sonicator for at least 30 minutes, mix the Acetone/particle mixture with SMP resin and then remove the Acetone through vacuum. This theoretically would solve the particle dispersion problem if the process could remove 100% of the Acetone; however, it is unknown how it would affect the result. This test is forthcoming to verify the effects.

7 Summary

This paper demonstrates the system level design of a novel reconfigurable system that integrates multi-functional structures and materials including energy harvesting. Direct utilization of thermal energy helps to decrease the losses associated with energy conversion and passive activation using thermal energy can reduce the weight penalty by eliminating complicated control systems and separate actuators.

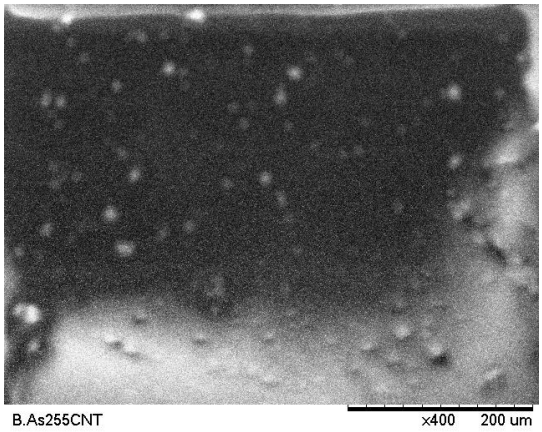

Fig. 11. SEM micrograph of 10 wt % magnetite in VeriflexE

References

[1] J. J. Joo, D. Robertson, B. M. Smyers, G. W. Reich, 2010, "Thermally-Activated Reconfigurable Wing Design Using a Non-Monolithic Compliant Mechanism", 51st AIAA/ASME/ASCE/AHSs/ASC Structures, Structural Dynamics & Materials Conference, April 12-15, AIAA 2010-2665, Orlando, Florida

[2] R. Beblo, D. Robertson, J. Joo, B. Smyers, G. Reich, 2010, "System Design and Modeling of a Thermally Activated Reconfigurable Wing", Proceedings of ASME SMASIS Conference, Sept 28 – Oct 1, SMASIS2010-3636, Philadelphia, PA

[3] F. Castro, K. K. Westbrook, J. Hermiller, D. U. Ahn, Y. Ding, H. J. Qi, 2011, "Time and Temperature Dependent Recovery of Epoxy-Based Shape Memory Polymers", Journal of Engineering Materials and Technology, vol. 133

[4] A.J.W. McClung, G.P. Tandon, J.W. Baur, 2010, "The Strain Rate and Temperature Dependent Mechanical Behavior of Veriflex-E in Tension", Proceedings of ASME SMASIS Conference, Sept 28 – Oct 1, SMASIS2010-3674, Philadelphia, PA

[5] Ki-iti Horai and G. Simmons, "Thermal Conductivity of Rock-Forming Minerals", Earth and Planetary Science Letters, vol. 6, pp 359-368, 1969

[6] J. Molgaard and W.W. Smeltzer, "Thermal Conductivity of Magnetite and Hematite", Journal of Applied Physics", vol. 42, no. 9, pp 3644-3647, 1971

[7] Clauser C, Huenges E. "Thermal conductivity of rocks and minerals", In: Ahrens TJ, editor. Rock physics and phase relations. A handbook of physical constants. American Geophysical Union Reference; 1995.

[8] Muhannad Yasar Razzaq, Mathias Anhalt, Lars Frormann, Bernd Weidenfeller, "Thermal, electrical and magnetic studies of magnetite filled polyurethane shape memory polymers", Materials Science and Engineering A, vol. 444, pp 227-235, 2007

[9] George S. Parks and Kenneth K. Kelley, "The Heat Capacities of Some Metallic Oxides", J. Phys. Chem. Vol. 30, no. 1, pp 47-55, 1926

[10] Edgar F. Westrum Jr, Fredrik Gronvold, "Magnetite (Fe3O4) Heat capacity and thermodynamic properties from 5 to 350 K, low-temperature transition", J. Chem. Thermodynamics, vol. 1, pp 543-557, 1969